DALTON

# Intramolecular electron transfer in linear trinuclear complexes of copper(I), silver(I) and gold(I) bound to redox-active cyanomanganese ligands*

**Nathan C. Brown,[a] Gene B. Carpenter,[b] Neil G. Connelly,[a] John G. Crossley,[a] Antonio Martín,[a] A. Guy Orpen,[a] Anne L. Rieger,[b] Philip H. Rieger[b] and Gillian H. Worth[a]**

[a] *School of Chemistry, University of Bristol, Bristol BS8 1TS, UK*
[b] *Department of Chemistry, Brown University, Providence, RI 02912, USA*

The reaction of $[Cu(NCMe)_4][PF_6]$ with 2 equivalents of $[Mn(CN)L_x]$ {$L_x$ = $(CO)(dppm)_2$, *cis*- or *trans*-$(CO)_2[P(OR)_3](dppm)$ (R = Ph or Et, dppm = $Ph_2PCH_2PPh_2$)} in $CH_2Cl_2$ gave $[Cu\{(\mu\text{-}NC)MnL_x\}_2][PF_6]$. With 2 equivalents of $[Mn(CN)L_x]$ in toluene, $AgPF_6$ gave $[Ag\{(\mu\text{-}NC)MnL_x\}_2]^+$ {$L_x$ = *cis*- or *trans*-$(CO)_2[P(OR)_3](dppm)$ (R = Ph or Et)} but in $CH_2Cl_2$ *cis*-$[Mn(CN)(CO)_2(PEt_3)(dppe)]$ (dppe = $Ph_2PCH_2CH_2PPh_2$) or *trans*-$[Mn(CN)(CO)(dppm)_2]$ and AgX (X = $BF_4^-$, $PF_6^-$ or $SbF_6^-$) gave the tricationic manganese(II) complexes $[Ag\{(\mu\text{-}NC)Mn(CO)(dppm)_2\}_2][PF_6]_3$ and $[Ag\{(\mu\text{-}NC)MnL_x\}_2]X_3$ {$L_x$ = *trans*-$(CO)_2(PEt_3)(dppe)$]; the complexes $[Ag\{(\mu\text{-}NC)MnL_x\}_2][PF_6]_3$ {$L_x$ = *trans*-$(CO)_2[P(OR)_3](dppm)$ (R = Ph or Et)} were prepared directly from $Ag[PF_6]$ and *trans*-$[Mn(CN)(CO)_2\{P(OR)_3\}(dppm)][PF_6]$ (R = Ph or Et) in $CH_2Cl_2$. Treatment of [AuCl(tht)] (tht = tetrahydrothiophene) with $[Mn(CN)L_x]$ in $CH_2Cl_2$ in the presence of $Tl[PF_6]$ yielded $[Au\{(\mu\text{-}NC)MnL_x\}_2][PF_6]$ {$L_x$ = $(CO)(dppm)_2$, *cis*- or *trans*-$(CO)_2[P(OR)_3](dppm)$ (R = Ph or Et)}. X-Ray structural studies on $[Ag\{(\mu\text{-}NC)MnL_x\}_2][PF_6]$ {$L_x$ = *trans*-$(CO)_2[P(OPh)_3](dppm)$}, $[Au\{(\mu\text{-}NC)MnL_x\}_2][PF_6]$ {$L_x$ = *trans*-$(CO)_2[P(OEt)_3](dppm)$}, and $[Ag\{(\mu\text{-}NC)MnL_x\}_2][PF_6]_3$ [$L_x$ = $(CO)(dppm)_2$] showed, in each case, near linear Mn–CN–M′–NC–Mn skeletons (M′ = Ag or Au); the Mn–P and P–substituent bond lengths are consistent with octahedral $Mn^I$ and $Mn^{II}$ centres in the monocations and trication respectively. Each of the complexes $[M'\{(\mu\text{-}NC)MnL_x\}_2][PF_6]$ {M′ = Cu or Au, $L_x$ = $(CO)(dppm)_2$; M′ = Cu or Ag, $L_x$ = *trans*-$(CO)_2[P(OR)_3](dppm)$ (R = Ph or Et)} showed one reversible two-electron oxidation wave at a platinum electrode in $CH_2Cl_2$; the trication $[Cu\{(\mu\text{-}NC)Mn(CO)(dppm)_2\}_2]^{3+}$ was generated in solution by controlled potential electrolysis of $[Cu\{(\mu\text{-}NC)Mn(CO)(dppm)_2\}_2]^+$, and $[Au\{(\mu\text{-}NC)Mn(CO)(dppm)_2\}_2][PF_6]_3$ was prepared by chemical oxidation of $[Au\{(\mu\text{-}NC)Mn(CO)(dppm)_2\}_2][PF_6]$ with $[Fe(cp)_2][PF_6]$ (cp = $\eta$-$C_5H_5$) in $CH_2Cl_2$. Magnetic and ESR spectroscopic studies provided further evidence for the presence of two isolated low-spin $Mn^{II}$ centres in the trications $[Ag\{(\mu\text{-}NC)MnL_x\}_2]^{3+}$ {$L_x$ = $(CO)(dppm)_2$, *trans*-$(CO)_2[P(OR)_3](dppm)$ (R = Ph or Et) or *trans*-$(CO)_2(PEt_3)(dppe)$}. By contrast, $[Au\{(\mu\text{-}NC)MnL_x\}_2]^+$ {$L_x$ = *trans*-$(CO)_2[P(OR)_3](dppm)$ (R = Et or Ph)} showed two reversible one-electron oxidation waves corresponding to the stepwise formation of di- and trications. Electrolytic oxidation of $[Au\{(\mu\text{-}NC)MnL_x\}_2]^+$ in tetrahydrofuran, or chemical oxidation with $[N(C_6H_4Br\text{-}p)_3]^+$ or $[Fe(\eta\text{-}C_5H_4COMe)(cp)]^+$ in $CH_2Cl_2$, gave solutions of $[Au\{(\mu\text{-}NC)MnL_x\}_2]^{2+}$ {$L_x$ = *trans*-$(CO)_2[P(OEt)_3](dppm)$}, IR spectroscopic and voltammetric studies on which are compatible with weak interaction between the two manganese centres in the mixed-valence dication.

When the octahedral cyanomanganese(I) complexes, $[Mn(CN)L_x]$ (Scheme 1), behave as redox-active ligands[1] the ability of the cyanide bridge to mediate intramolecular electron transfer to an N-bound metal site [M′ in $L_xMn(\mu\text{-}CN)M'$] can depend on the geometric arrangement of the ancillary ligands, $L_x$, at manganese; ESR spectroscopy and extended-Hückel molecular orbital (EHMO) studies have shown that the singly occupied molecular orbitals (SOMOs) of *trans*-$[Mn(CN)(CO)(dppm)_2]^+$ (dppm = $Ph_2PCH_2PPh_2$) and *trans*-$[Mn(CN)(CO)_2L(dppm)]^+$ have δ and π symmetry respectively with respect to the Mn–CN axis.[2] Thus, when complexes such as $[L_n(OC)_{5-n}Mn(\mu\text{-}CN)ML'_y]$ undergo one-electron oxidation at Mn, interaction between Mn and M′ through the CN bridge would be favoured by the ligand *trans*-$[Mn(CN)(CO)_2L(dppm)]^+$ but not by *trans*-$[Mn(CN)(CO)(dppm)_2]^+$.

Supporting evidence for such ligand-set control of intramolecular electron transfer is provided by electrochemical studies of the heterotrinuclear complexes $[Rh(CO)_2\{(\mu\text{-}NC)MnL_x\}_2][PF_6]$ {$L_x$ = *trans*-$(CO)_2[P(OR)_3](dppm)$ (R = Et or Ph) *cis* geometry at square planar $Rh^I$}; two closely spaced one-electron oxidation waves ($\Delta E^{o\prime}$ = *ca.* 80–90 mV) suggest weak but detectable communication between the two Mn sites.[3] Arguing that the extent of communication between two redox-active cyanomanganese ligands would be enhanced by their mutual *trans* arrangement at M′, we sought to synthesise linear heterotrinuclear species and study their electrochemical properties as a probe of the electronic communication through M′. We now describe complexes in which two Mn(CN) ligands are linearly bound as donors to copper(I), silver(I) and gold(I), and provide evidence to suggest that intramolecular electron transfer depends not only on the arrangement of the ancillary ligands at manganese but also on the identity of the Lewis acidic metal.

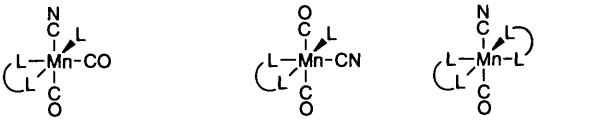


$L_x$ = *cis*-$(CO)_2[P(OR)_3](dppm)$ (R = Et or Ph) or *cis*-$(CO)_2(PEt_3)(dppe)$ | $L_x$ = *trans*-$(CO)_2[P(OR)_3]$-(dppm) (R = Et or Ph) | $L_x$ = $(CO)(dppm)_2$

**Scheme 1** The cyanomanganese ligands $[Mn(CN)L_x]$

* *Non-SI unit employed:* $\mu_B \approx 9.274 \times 10^{-24}$ J $T^{-1}$.

## Results and Discussion

### Synthesis of manganese(I) complexes

Treatment of $[Cu(NCMe)_4][PF_6]$ in $CH_2Cl_2$ with 2 equivalents of a cyanomanganese ligand, $Mn(CN)L_x$, rapidly results in the displacement of all four acetonitrile ligands and the formation of a yellow solution from which yellow or orange solids, characterised by elemental analysis, IR spectroscopy and mass spectrometry (Table 1) as $[Cu\{(\mu\text{-}NC)MnL_x\}_2][PF_6]$ {$L_x$ = *cis*- or *trans*-$(CO)_2[P(OR)_3]$(dppm) (R = Ph or Et) or $(CO)(dppm)_2$}, can be isolated in good yield. Nitrogen co-ordination of the cyanomanganese ligand to copper results in a shift to higher energy, and an increase in intensity, of the cyanide stretching vibration. The energy is also dependent on the ancillary ligand set ($L_x$) on Mn such that ν(CN) decreases in the order $L_x$ = *cis*-$(CO)_2[P(OPh)_3]$(dppm) > *cis*-$(CO)_2[P(OEt)_3]$(dppm) > *trans*-$(CO)_2[P(OPh)_3]$(dppm) > *trans*-$(CO)_2[P(OEt)_3]$(dppm) ≥ $(CO)(dppm)_2$. For a given phosphite the *cis* ligand set, in which the CN bridge is *trans* to a CO ligand, gives rise to a higher energy cyanide stretching vibration than the *trans* ligand set where the cyanide is *trans* to one of the phosphorus atoms of dppm.

Similar trends are observed in the IR spectra of analogous silver and gold complexes (Table 1). The former were prepared as pale yellow solids by adding $AgPF_6$ to 2 equivalents of $Mn(CN)L_x$ in toluene. However, when the same reactions were carried out with *cis*- or *trans*-$[Mn(CN)(CO)_2\{P(OR)_3\}(dppm)]$ (R = Ph or Et) in $CH_2Cl_2$ mixtures were formed which contained both the $Mn^I$ complex $[Ag\{(\mu\text{-}NC)MnL_x\}_2]^+$ {$L_x$ = *cis*- or *trans*-$(CO)_2[P(OR)_3]$(dppm) (R = Ph or Et)} and the tricationic complex $[Ag\{(\mu\text{-}NC)MnL_x\}_2]^{3+}$ {$L_x$ = *trans*-$(CO)_2[P(OR)_3]$(dppm) (R = Ph or Et)} the product of both N-co-ordination at silver and oxidation of both $Mn^I$ centres to $Mn^{II}$. Moreover, treatment of *cis*-$[Mn(CN)(CO)_2(PEt_3)(dppe)]$ (dppe = $Ph_2PCH_2CH_2PPh_2$) with AgX (X = $BF_4^-$, $PF_6^-$ or $SbF_6^-$) in $CH_2Cl_2$ gave only the deep purple salts $[Ag\{(\mu\text{-}NC)MnL_x\}_2]X_3$ {$L_x$ = *trans*-$(CO)_2(PEt_3)(dppe)$] (see below). We have pointed out previously[4] that the ability of $Ag^I$ salts to act as one-electron oxidants is strongly solvent dependent. Here, complexation of the silver(I) ion by toluene yields a much weaker oxidant than that found in the non-co-ordinating solvent $CH_2Cl_2$. Thus, striking and selective routes to either the reduced or oxidised forms of the heterotrinuclear silver(I) complexes of the dicarbonylmanganese ligands result, simply by varying the solvent.

The monocarbonyl complex *trans*-$[Mn(CN)(CO)(dppm)_2]$ is the most readily oxidised of the cyanomanganese ligands. Accordingly, its reaction with $Ag[PF_6]$ gives only the tricationic complex $[Ag\{(\mu\text{-}NC)Mn(CO)(dppm)_2\}_2][PF_6]_3$; no route to the monocationic complex $[Ag\{(\mu\text{-}NC)Mn(CO)(dppm)_2\}_2][PF_6]$ has been found.

The yellow complexes of gold, $[Au\{(\mu\text{-}NC)MnL_x\}_2][PF_6]$ {$L_x$ = *cis*- or *trans*-$(CO)_2[P(OR)_3]$(dppm) (R = Ph or Et) or $(CO)(dppm)_2$}, are also readily prepared in good yield, by treating [AuCl(tht)] (tht = tetrahydrothiophene) with $[Mn(CN)L_x]$ in $CH_2Cl_2$. On adding 1 equivalent of the cyanomanganese ligand, tht is displaced to give a solution of $[AuCl\{(\mu\text{-}NC)MnL_x\}]$; addition of the second equivalent of the ligand and treatment of the mixture with $Tl[PF_6]$ leads to halide abstraction and the isolation of the trinuclear monocation.

Although the spectroscopic and analytical data presented in Table 1 characterise the stoichiometry and geometrical arrangement of the ligands about the $Mn^I$ centres of $[M'\{(\mu\text{-}NC)MnL_x\}_2]^+$ (M' = Cu, Ag or Au), X-ray structural studies were carried out on representative silver and gold complexes in order to define the detailed geometry, linear or otherwise, of the Mn(μ-CN)M'(μ-NC)Mn skeleton.

### Crystal structures of $[Ag\{(\mu\text{-}NC)MnL_x\}_2][PF_6]$ {$L_x$ = *trans*-$(CO)_2[P(OPh)_3]$(dppm)} and $[Au\{(\mu\text{-}NC)MnL_x\}_2][PF_6]$ {$L_x$ = *trans*-$(CO)_2[P(OEt)_3]$(dppm)}

Crystals of $[Ag\{(\mu\text{-}NC)MnL_x\}_2][PF_6]$ {$L_x$ = *trans*-$(CO)_2[P(OPh)_3]$(dppm)} (as its diethyl ether solvate) and $[Au\{(\mu\text{-}NC)MnL_x\}_2][PF_6]$ {$L_x$ = *trans*-$(CO)_2[P(OEt)_3]$(dppm)} (as its $CH_2Cl_2$ solvate) were grown by allowing a concentrated $CH_2Cl_2$ solution of the complex to diffuse into diethyl ether and *n*-hexane respectively at −10 °C. The structures of the cations are shown in Figs. 1 and 2 and selected bond lengths and angles are given in Tables 2 and 3.

The silver complex contains two essentially octahedral manganese(I) cyanide ligands linearly bound to $Ag^I$ (N–Ag–N 180°); the two halves of the cation are related by a crystallographically imposed centre of inversion, at the silver atom. The Mn–CN–Ag unit is also nearly linear [Mn–C–N 174.7(7), Ag–N–C 168.2(7) Å] and, as inferred from the IR spectrum, the two carbonyl ligands bound to each manganese atom are mutually *trans* disposed.

No detailed comparison can be made between the structures of $[Ag\{(\mu\text{-}NC)MnL_x\}_2][PF_6]$ {$L_x$ = *trans*-$(CO)_2[P(OPh)_3]$(dppm)} and $[Au\{(\mu\text{-}NC)MnL_x\}_2][PF_6]$ {$L_x$ = *trans*-$(CO)_2[P(OEt)_3]$(dppm)} because of the limited precision of the structure determinations and because the phosphite ligand substituents are different. Nevertheless, the geometry of $[Au\{(\mu\text{-}NC)MnL_x\}_2]^+$ {$L_x$ = *trans*-$(CO)_2[P(OEt)_3]$(dppm)} is very similar to that of $[Ag\{(\mu\text{-}NC)MnL_x\}_2]^+$ {$L_x$ = *trans*-$(CO)_2[P(OPh)_3]$(dppm)} in most respects (although there is no crystallographically imposed centre of symmetry in the gold complex); the arrangement of the ligands about each manganese atom is the same and the Mn–CN–Au–NC–Mn skeleton is again nearly linear [N–Au–N 176.7(9), Mn–C–$N_{ave}$ 179(6), Au–N–$C_{ave}$ 174(2)°]. The most striking difference in the solid-state structures is that the $P(OR)_3$–Mn ··· Mn–$P(OR)_3$ moiety in the silver species is strictly transoid (P–Mn ··· Mn–P dihedral angle 180° by symmetry) whereas that in the gold cation is cisoid (P–Mn ··· Mn–P dihedral angle 26.5°).

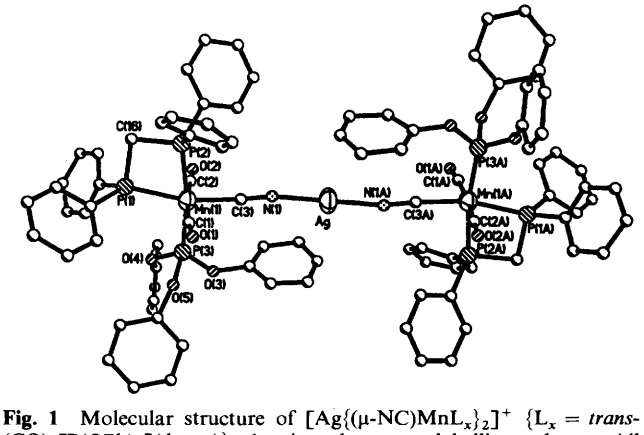


**Fig. 1** Molecular structure of $[Ag\{(\mu\text{-}NC)MnL_x\}_2]^+$ {$L_x$ = *trans*-$(CO)_2[P(OPh)_3]$(dppm)} showing the atom labelling scheme. All hydrogen atoms have been omitted for clarity

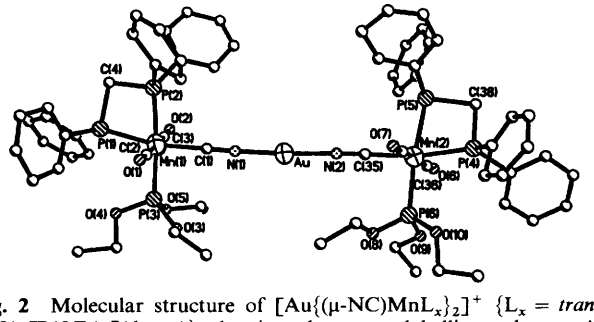


**Fig. 2** Molecular structure of $[Au\{(\mu\text{-}NC)MnL_x\}_2]^+$ {$L_x$ = *trans*-$(CO)_2[P(OEt)_3]$(dppm)} showing the atom labelling scheme. All hydrogen atoms have been omitted for clarity

**Table 1** Analytical and IR spectroscopic data for the complexes $[M'\{(\mu\text{-}NC)MnL_x\}_2]^{z+}$ [a]

| M | $L_x$ | z | Colour | Yield (%) | Analysis[b] (%) C | H | N | IR[c]/cm$^{-1}$ ν(CN) | ν(CO)[e] | $E^{o'}$[d]/V | m/z | $\mu_{eff}/\mu_B$ |
|---|---|---|---|---|---|---|---|---|---|---|---|---|
| Cu | *cis*-$(CO)_2[P(OPh)_3]$(dppm) | 1 | Pale yellow | 67 | 59.0 (59.0) | 3.7 (4.0) | 1.5 (1.5) | 2123w | 1976s, 1926s | 1.44I (0.96) | — | — |
| Cu | *trans*-$(CO)_2[P(OPh)_3]$(dppm) | 1 | Yellow | 73 | 58.5 (59.0) | 4.3 (4.0) | 1.7 (1.5) | 2108mw | 1939s (2019) | 1.02 | 1725 | — |
| Cu | *cis*-$(CO)_2[P(OEt)_3]$(dppm) | 1 | Yellow | 65 | 51.2 (51.6) | 4.8 (4.7) | 1.6 (1.8) | 2118w | 1964s, 1912s | 1.30I (0.74) | — | — |
| Cu | *trans*-$(CO)_2[P(OEt)_3]$(dppm) | 1 | Yellow | 78 | 52.0 (51.6) | 5.1 (4.7) | 1.8 (1.8) | 2096mw | 1926s (2008) | 0.82 | 1437 | — |
| Cu | *trans*-$(CO)(dppm)_2$ | 1 | Orange | 71 | 63.8 (63.6) | 4.7 (4.5) | 1.8 (1.4) | 2092mw | 1879s | 0.34 | 1817 | — |
| Ag | *cis*-$(CO)_2[P(OPh)_3]$(dppm) | 1 | Pale yellow | 61 | 57.7 (57.7) | 4.1 (3.9) | 1.4 (1.5) | 2121w | 1977s, 1925s | 1.42I (0.93) | — | — |
| Ag | *trans*-$(CO)_2[P(OPh)_3]$(dppm) | 1 | Yellow | 75 | 57.8 (57.7) | 4.0 (3.9) | 1.4 (1.5) | 2106mw | 1937s (2018) | 0.97 | — | — |
| Ag | *trans*-$(CO)_2[P(OEt)_3]$(dppm) | 1 | Pale yellow | 67 | 50.4 (50.2) | 4.6 (4.6) | 1.5 (1.7) | 2096mw | 1925s (2007) | 0.79 | 1483 | — |
| Ag | *trans*-$(CO)_2[P(OPh)_3]$(dppm) | 3 | Blue | 61 | 49.2 (48.8) | 3.4 (3.3) | 1.2 (1.2)[f] | 2141w | 2008vs (2076) | 0.98 | — | 3.35 |
| Ag | *trans*-$(CO)_2[P(OEt)_3]$(dppm) | 3 | Purple | 51 | 43.1 (42.6) | 4.3 (3.9) | 1.4 (1.5) | 2143w | 2001vs (2071) | 0.77 | — | 2.90 |
| Ag | *trans*-$(CO)_2(PEt_3)$(dppe) | 3 | Purple | 33 | 42.9 (42.8) | 4.2 (4.1) | 1.5 (1.4)[g] | 2139w | 1979s | — | — | 3.02 |
| Ag | *trans*-$(CO)_2(PEt_3)$(dppe)[h] | 3 | Purple | 30 | 48.9 (49.6) | 4.7 (4.6) | 1.8 (1.6)[i] | 2140w | 1978s (2047) | — | — | — |
| Ag | *trans*-$(CO)_2(PEt_3)$(dppe)[j] | 3 | Purple | 37 | 39.4 (39.6) | 3.6 (3.7) | 1.3 (1.3) | 2140w | 1979s | — | — | 2.87 |
| Ag | *trans*-$(CO)(dppm)_2$ | 3 | Deep red | 41 | 54.2 (54.4) | 3.8 (3.9) | 1.2 (1.2) | 2124w | 1947s | 0.32 | — | 2.99 |
| Au | *cis*-$(CO)_2[P(OPh)_3]$(dppm) | 1 | Pale yellow | 74 | 53.7 (53.4) | 3.8 (3.7) | 1.5 (1.3)[f] | 2133mw | 1978s, 1928s | 1.54I (0.68, 0.97) | — | — |
| Au | *trans*-$(CO)_2[P(OPh)_3]$(dppm) | 1 | Yellow | 58 | 54.7 (55.1) | 3.6 (3.7) | 1.3 (1.4) | 2114m | 1940vs (2023) | 0.82, 1.09 | — | — |
| Au | *cis*-$(CO)_2[P(OEt)_3]$(dppm) | 1 | Pale yellow | 58 | 46.3 (46.0) | 4.4 (4.3) | 1.6 (1.6)[f] | 2126w | 1965s, 1914s | 1.35I (0.54, 0.82) | — | — |
| Au | *trans*-$(CO)_2[P(OEt)_3]$(dppm) | 1 | Yellow | 56 | 47.8 (47.6) | 4.1 (4.3) | 1.4 (1.6) | 2101m | 1926s (2010) | 0.64, 0.92 | — | — |
| Au | *trans*-$(CO)_2[P(OEt)_3]$(dppm)[k] | 2 | — | — | — | — | — | 2163, 2096; 2165, 2091[l] | 2004, 1928; 2001, 1931[l] | — | — | — |
| Au | *trans*-$(CO)_2[P(OEt)_3]$(dppm)[k] | 3 | — | — | — | — | — | 2174w | 2006s (2077) | — | — | — |
| Au | *trans*-$(CO)(dppm)_2$ | 1 | Orange | 59 | 59.5 (59.6) | 4.5 (4.2) | 1.1 (1.3) | 2102m | 1881s | 0.34 | — | — |
| Au | *trans*-$(CO)(dppm)_2$ | 3 | Red | 73 | 51.4 (51.5) | 3.8 (3.5) | 0.9 (1.2) | 2135mw | 1954s | 0.34 | — | — |

[a] Isolated as $[PF_6]^-$ salts unless stated otherwise. [b] Calculated values in parentheses. [c] In $CH_2Cl_2$; s = strong, m = medium, w = weak absorption. [d] $E^{o'}$ for reversible wave unless otherwise stated. The oxidation peak potential, $(E_p)_{ox}$, at a scan rate of 200 mV s$^{-1}$, is given for an irreversible (I) wave; numbers in parentheses are $(E_p)_{red}$, at a scan rate of 200 mV s$^{-1}$, for the reversible product wave. [e] Very weak A-mode given in parentheses. [f] Sample analysed as a 1.0 $CH_2Cl_2$ solvate. [g] Sample analysed as a 2.0 $CH_2Cl_2$ solvate. [h] $[BF_4]^-$ salt. [i] Sample analysed as a 0.5 $CH_2Cl_2$ solvate. [j] $[SbF_6]^-$ salt. [k] Not isolated, see text. [l] The first two bands are those observed after chemical oxidation of the monocation in $CH_2Cl_2$, the second after controlled potential electrolysis of the monocation in tetrahydrofuran (thf)(see text).

**Table 2** Selected bond lengths (Å) and angles (°) for $[Ag\{(\mu\text{-}NC)MnL_x\}_2][PF_6]$ $\{L_x$ = *trans*-$(CO)_2[P(OPh)_3]$(dppm)$\}$ *

| | | | |
|---|---|---|---|
| Ag–N | 2.059(7) | Mn–C(N) | 1.932(8) |
| C–N | 1.150(9) | Mn–P(OPh) | 2.184(2) |
| $Mn–C(O)_{ave}$ | 1.815(10) | | |
| N–Ag–N | 180.0 | Ag–N–C | 168.2(7) |
| Mn–C–N | 174.7(7) | | |

* As its 1 : 2 diethyl ether solvate.

**Table 3** Selected bond lengths (Å) and angles (°) for $[Au\{(\mu\text{-}NC)MnL_x\}_2][PF_6]$ $\{L_x$ = *trans*-$(CO)_2[P(OEt)_3]$(dppm)$\}$ *

| | | | |
|---|---|---|---|
| $Au–N_{ave}$ | 2.01(2) | $Mn–C(N)_{ave}$ | 1.95(3) |
| $C–N_{ave}$ | 1.115(20) | $Mn–P(OEt)_{ave}$ | 2.234(10) |
| $Mn–C(O)_{ave}$ | 1.77(4) | | |
| N–Au–N | 176.7(9) | $Au–N–C_{ave}$ | 174(2) |
| $Mn–C–N_{ave}$ | 179(6) | | |

* As its 1 : 1.25 $CH_2Cl_2$ solvate.

However, it is difficult to imagine a significant barrier to rotation about the Mn–CN–M′–NC–Mn axis in these species in solution. There is, therefore, no obvious structural difference which might account for the very different electrochemical behaviour of the two cations (see below).

## Electrochemistry of trinuclear manganese(I) complexes

Cyclic voltammetry at a platinum electrode in $CH_2Cl_2$ shows that each of the $Cu^I$, $Ag^I$ and $Au^I$ complexes undergoes oxidation in the potential range 0.0–1.8 V (Table 1); for the copper and gold complexes no reduction waves are observed (to −1.8 V) but for each silver complex an irreversible wave, with a very high current, is observed at *ca.* −1.2 V.

The most readily oxidised complexes, namely $[M'\{(\mu\text{-}NC)Mn(CO)(dppm)_2\}_2][PF_6]$ (M′ = Cu or Au), show one reversible wave $[(i_p)_{red}/(i_p)_{ox} = 1.0$ for scan rates from 50 to 200 mV s$^{-1}$] centred at 0.34 V. Exhaustive electrolysis, at 0.50 V, of the yellow copper compound in $CH_2Cl_2$ resulted in the formation of an orange-red solution (showing IR carbonyl and cyanide absorptions at 1952 and 2122 cm$^{-1}$ respectively) and coulometry confirmed the loss of 1.96 electrons per cation, *i.e.* the oxidation wave corresponds to a two-electron process, one-electron oxidation at both $Mn^I$ centres. The cyclic and rotating platinum voltammograms of the product solution also confirmed the presence of the trication $[Cu\{(\mu\text{-}NC)\text{-}Mn(CO)(dppm)_2\}_2]^{3+}$ {though the observation of a small reduction wave at *ca.* 0.03 V, in addition to the main wave at 0.34 V, suggested the formation of some of the free monocation *trans*-$[Mn(CN)(CO)(dppm)_2]^+$}.

The cyclic voltammograms of the trinuclear species containing *cis*-$[Mn(CN)(CO)_2L(L\text{–}L)]$ [L–L = dppm, L = $P(OR)_3$ (R = Ph or Et); L–L = dppe, L = $PEt_3$] as ligands are complicated by the oxidative isomerisation process observed for all such units;[5] irreversible oxidation waves are coupled with product waves associated with the formation of

*trans*-$[Mn^{II}(CN)(CO)_2L(L–L)]$ centres. However, the copper and silver complexes $[M\{(\mu\text{-NC})MnL_x\}_2]^+$ {M = Cu or Ag, $L_x$ = *trans*-$(CO)_2[P(OR)_3]$(dppm) (R = Ph or Et)} show uncomplicated voltammograms with one reversible two-electron oxidation wave corresponding to the formation of the trications $[M\{(\mu\text{-NC})MnL_x\}_2]^{3+}$. The potential for this process, in the range 0.79–1.02 V (Table 1) depends in the expected manner on the ligand set, $L_x$; each wave is shifted to a more positive potential than that of the free cyanomanganese ligand.

The voltammetry of the gold complexes $[Au\{(\mu\text{-NC})MnL_x\}_2]^+$ {$L_x$ = *cis*- or *trans*-$(CO)_2[P(OR)_3]$(dppm) (R = Et or Ph)} is strikingly different from that of the copper and silver analogues. While each of $[Au\{(\mu\text{-NC})MnL_x\}_2]^+$ {$L_x$ = *cis*-$(CO)_2[P(OR)_3]$(dppm) (R = Et or Ph)} does show one irreversible oxidation wave, at a potential similar to those observed for the Cu and Ag analogues, it is accompanied in each case by *two* product reduction waves, at 0.68 and 0.97 (R = Ph) and 0.54 and 0.82 V (R = Et) respectively. That both waves are due to the formation of only one product is shown by the cyclic voltammetry of $[Au\{(\mu\text{-NC})MnL_x\}_2]^+$ {$L_x$ = *trans*-$(CO)_2[P(OR)_3]$(dppm) (R = Et or Ph)} each of which shows two reversible oxidation waves. The potentials of these waves are different from that of the one wave observed for each of the copper and silver analogues; perhaps coincidentally, the average of the potentials for the two waves is approximately the same as the potential for the oxidation of the copper and silver complexes.

Each of the two waves for $[Au\{(\mu\text{-NC})MnL_x\}_2]^+$ {$L_x$ = *trans*-$(CO)_2[P(OR)_3]$(dppm) (R = Et or Ph)} is approximately half the height of the single oxidation wave of the copper or silver analogue (studied at the same concentration). Assuming the diffusion coefficients of analogous copper, silver and gold complexes to be similar, the voltammetric data suggest that whereas the copper and silver complexes undergo two-electron oxidation (confirmed by the electrolytic oxidation of $[Cu\{(\mu\text{-NC})Mn(CO)(dppm)_2\}_2]^+$ to the trication, see above), each of the gold analogues is oxidised in two sequential one-electron steps, to di- and tri-cations. In order to confirm this suggestion, controlled potential oxidation of $[Au\{(\mu\text{-NC})MnL_x\}_2]^+$ {$L_x$ = *trans*-$(CO)_2[P(OEt)_3]$(dppm)} was carried out at 0.85 V in thf under argon. (Electrode coating hampered the experiment in $CH_2Cl_2$; the voltammetry of the complex was qualitatively the same in thf and $CH_2Cl_2$.) After the loss of one electron per monocation ($n$ = 1.0), cyclic and rotating platinum electrode voltammetry of the resulting dark yellow solution showed one reduction wave at 0.72 V and one oxidation wave at 0.98 V, as expected for the formation of the dication $[Au\{(\mu\text{-NC})MnL_x\}_2]^+$ {$L_x$ = *trans*-$(CO)_2[P(OEt)_3]$(dppm)}; the nature of this complex is discussed below.

### Chemical oxidation of trinuclear manganese(I) complexes containing the ligand *trans*-[Mn(CN)(CO)(dppm)$_2$]

The chemical oxidation of the complexes $[M\{(\mu\text{-NC})MnL_x\}_2]^+$ (M = Cu, Ag or Au) was investigated on the basis of the voltammetric and electrolytic studies described above. The copper complexes are particularly prone to dissociation to mononuclear products on oxidation, suggesting the Cu–N bonds in the products are less robust than analogous Ag–N and Au–N bonds (see below).

The low potential, 0.34 V, at which the complexes $[M\{(\mu\text{-NC})Mn(CO)(dppm)_2\}_2][PF_6]$ (M = Cu or Au) undergo two-electron oxidation suggested that the corresponding trications would be readily accessible using mild oxidants. Treatment of $[Au\{(\mu\text{-NC})Mn(CO)(dppm)_2\}_2][PF_6]$ with 2 equivalents of $[Fe(cp)_2][PF_6]$ (cp = $\eta$-$C_5H_5$) in $CH_2Cl_2$ resulted in a colour change from orange to red and a shift in $\nu$(CO) of *ca.* 70 $cm^{-1}$ to higher energy, as expected for oxidation of both $Mn^I$ centres to $Mn^{II}$; treatment of the reaction mixture with *n*-hexane gave a good yield of $[Au\{(\mu\text{-NC})Mn(CO)(dppm)_2\}_2][PF_6]_3$ as a red solid (Table 1). This complex was readily characterised by elemental analysis and by the observation of one reduction wave at 0.34 V, identical to the potential for the oxidation of $[Au\{(\mu\text{-NC})Mn(CO)(dppm)_2\}_2][PF_6]$. In accord with the oxidation of the C-bound end of the Mn(μ-CN)Au fragment, $\nu$(CN) is shifted to higher energy, from 2102 to 2135 $cm^{-1}$, on oxidation.

The reaction of $[Cu\{(\mu\text{-NC})Mn(CO)(dppm)_2\}_2][PF_6]$ with $[Fe(cp)_2][PF_6]$ also gave a red solution but IR spectroscopy revealed the formation mainly of the uncomplexed cation *trans*-$[Mn(CN)(CO)(dppm)_2]^+$. Little evidence was found for the trinuclear tricationic copper complex even though it was detected voltammetrically in solution after electrolytic oxidation of $[Cu\{(\mu\text{-NC})Mn(CO)(dppm)_2\}_2][PF_6]$ (see above). Moreover, $[Cu\{(\mu\text{-NC})Mn(CO)(dppm)_2\}_2][PF_6]_3$ is not formed from *trans*-$[Mn(CN)(CO)(dppm)_2\}_2][PF_6]$ and $[Cu(NCMe)_4][PF_6]$.

As noted above, the silver complex $[Ag\{(\mu\text{-NC})Mn(CO)(dppm)_2\}_2][PF_6]$ cannot be prepared from *trans*-$[Mn(CN)(CO)(dppm)_2]$ and $Ag[PF_6]$. Rather, this reaction (carried out using a 1:3 ratio of the reactants) directly gives the deep red salt $[Ag\{(\mu\text{-NC})Mn(CO)(dppm)_2\}_2][PF_6]_3$. The IR spectrum of this trication is similar to that of the gold analogue (Table 1) and the cyclic voltammogram in $CH_2Cl_2$ shows a reduction wave at 0.32 V {albeit accompanied by a smaller wave at 0.06 V due to the presence of uncomplexed *trans*-$[Mn(CN)(CO)(dppm)_2]^+$}.

The voltammetry of $[M\{(\mu\text{-NC})Mn(CO)(dppm)_2\}_2][PF_6]$ (M = Cu or Au) and $[Ag\{(\mu\text{-NC})Mn(CO)(dppm)_2\}_2][PF_6]_3$ implied that the monocation is oxidised in a single two-electron step, affording a trication containing two non-interacting $Mn^{II}$ centres. Such behaviour is consistent with our earlier studies which suggested that the SOMO of *trans*-$[Mn(CN)(CO)(dppm)_2]^+$ has the incorrect symmetry to sustain intramolecular electron transfer through the cyanide bridge.[2] Magnetic studies provide direct support for this suggestion in that the anisotropic ESR spectrum of $[Ag\{(\mu\text{-NC})Mn(CO)(dppm)_2\}_2][PF_6]_3$ [in $CH_2Cl_2$–thf (2:1), at 77 K] is virtually identical to that[2] of *trans*-$[Mn(CN)(CO)(dppm)_2]^+$ and the room temperature magnetic moment of the solid paramagnetic salt ($\mu_{eff}$ = 2.99 $\mu_B$) confirms the presence of two unpaired electrons, *i.e.* of two isolated low spin $Mn^{II}$ centres. Further support is provided by the crystal structure of $[Ag\{(\mu\text{-NC})Mn(CO)(dppm)_2\}_2][PF_6]_3$.

### Crystal structure of $[Ag\{(\mu\text{-NC})MnL_x\}_2][PF_6]_3$ [$L_x$ = (CO)(dppm)$_2$]

Crystals of $[Ag\{(\mu\text{-NC})Mn(CO)(dppm)_2\}_2][PF_6]_3$, as its $CH_2Cl_2$ solvate, were grown from degassed, layered $CH_2Cl_2$–cyclohexane under anaerobic conditions at −10 °C to give air- and light-sensitive crystals. The crystal was mounted in a thin-walled capillary containing a little solvent and the capillary sealed. The molecular structure of the trication $[Ag\{(\mu\text{-NC})Mn(CO)(dppm)_2\}_2]^{3+}$ is shown in Fig. 3 and selected bond lengths and angles are given in Table 4. As in the monocationic silver complex described above, the geometry about the silver ion is linear (N–Ag–N 180°) (there is again a crystallographically imposed centre of symmetry) and that about each manganese atom is essentially octahedral. The most significant structural parameters, however, are the average Mn–P [2.349(6) Å] and P–$C_{ipso}$ (1.803 Å) distances and C–P–C angles (106.4°) which are closer to those of *trans*-$[Mn(CN)(CO)(dppm)_2]^+$ (Mn–P 2.346 Å, P–$C_{ipso}$ 1.813 Å, C–P–$C_{ave}$ 106.8°) than to those of *trans*-$[Mn(CN)(CO)(dppm)_2]$ (Mn–P 2.270 Å, P–$C_{ipso}$ 1.832 Å, C–P–$C_{ave}$ 104.3°)[2] and therefore diagnostic of two $Mn^{II}$ centres bound to silver(I) in $[Ag\{(\mu\text{-NC})Mn(CO)(dppm)_2\}_2]^{3+}$.

Despite the poor precision of the structures, a qualitative comparison can also be made between $[Ag\{(\mu\text{-NC})Mn$-

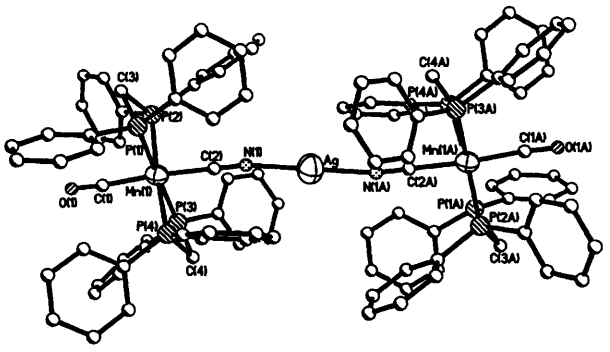

**Fig. 3** Molecular structure of $[Ag\{(\mu\text{-NC})Mn(CO)(dppm)_2\}_2]^{3+}$ showing the atom labelling scheme. All hydrogen atoms have been omitted for clarity

**Table 4** Selected bond lengths (Å) and angles (°) for $[Ag\{(\mu\text{-NC})Mn(CO)(dppm)_2\}_2][PF_6]_3$ *

| | | | |
|---|---|---|---|
| Ag–N | 2.18(3) | Mn–C(N) | 1.90(4) |
| C–N | 1.06(4) | $Mn–P_{ave}$ | 2.349(6) |
| $Mn–C(O)_{ave}$ | 1.87(4) | | |
| N–Ag–N | 180 | Ag–N–C | 166(2) |
| Mn–C–N | 179(2) | | |

* As its 1:4 $CH_2Cl_2$ solvate.

$(CO)(dppm)_2\}_2]^{3+}$ and $[Ag\{(\mu\text{-NC})MnL_x\}_2]^+$ $\{L_x$ = *trans*-$(CO)_2[P(OPh)_3](dppm)\}$, bearing in mind the different donor sets at manganese. Thus, in the trication the Ag–N distance [2.18(3) Å] is 0.12 Å longer than in the monocation; the differences reflect the relatively low level of manganese back donation to the cyanide π* orbitals in the $Mn^{II}$ complex, resulting in a less nucleophilic cyanide nitrogen atom (even though the ancillary ligands at the $Mn^{II}$ centre are more donating than those at $Mn^{I}$).

Comparisons can also be made with the structures of simple nitrile silver complexes. The HCN ligands in $[Ag(NCH)_2]^+$ are co-ordinated linearly to silver (N–Ag–N 180°) with a $Ag–N_{ave}$ distance of 2.130(3) Å,[6] and the structures of the linear polymer $[Ag_n(NCS)_{2n}]^{n+}$ [7] and $[Ag(NCCl)_2]^+$ [8] show Ag–N distances of 2.117(6) and 2.140(4) Å respectively. These distances are 0.06–0.08 Å longer than that of $[Ag\{(\mu\text{-NC})MnL_x\}_2]^+$ $\{L_x$ = *trans*-$(CO)_2[P(OPh)_3](dppm)\}$ and *ca.* 0.05 Å shorter than that of $[Ag\{(\mu\text{-NC})Mn(CO)(dppm)_2\}_2]^{3+}$, suggesting that the σ-donating (or π-accepting) ability of the nitrogen ligand towards silver decreases in the order $Mn^{I}(CN)$ > RCN (R = S, Cl or H) > $Mn^{II}(CN)$.

### Synthesis of trinuclear manganese(II) complexes containing the ligands *trans*-$[Mn(CN)(CO)_2L(L–L)]^+$

The magnitudes of the oxidation potentials (Table 1) of $[M\{(\mu\text{-NC})MnL_x\}_2]^+$ {M = Cu or Ag, $L_x$ = *trans*-$(CO)_2[P(OR)_3](dppm)$ (R = Et or Ph)} (0.79–1.02 V) suggest the need for oxidants stronger than the ferrocenium ion to bring about the formation of $[M\{(\mu\text{-NC})MnL_x\}_2]^{3+}$. Accordingly the monocations were treated with either $[NO]^+$ or $[N(C_6H_4Br\text{-}p)_3]^+$. The oxidation of the copper complexes led mainly to the formation of the uncomplexed cation *trans*-$[Mn(CN)(CO)_2\{P(OR)_3\}(dppm)]^+$. However, the tricationic silver complexes are much more stable and have been fully characterised (Table 1). As noted above, the reaction between *cis*- or *trans*-$[Mn(CN)(CO)_2\{P(OR)_3\}(dppm)]$ and $Ag[PF_6]$ in $CH_2Cl_2$ gives mixtures of $[Ag\{(\mu\text{-NC})MnL_x\}_2]^+$ $\{L_x$ = *cis*- or *trans*-$(CO)_2[P(OR)_3](dppm)$ (R = Et or Ph)} and $[Ag\{(\mu\text{-NC})MnL_x\}_2]^{3+}$ $\{L_x$ = *trans*-$(CO)_2[P(OR)_3](dppm)$ (R = Et or Ph)} whereas *cis*-$[Mn(CN)(CO)_2(PEt_3)(dppe)]$ gives a good yield of the purple salt $[Ag\{(\mu\text{-NC})MnL_x\}_2]^{3+}$ $[L_x$ = *trans*-$(CO)_2(PEt_3)(dppe)]$ directly. Pure samples of $[Ag\{(\mu\text{-NC})MnL_x\}_2][PF_6]_3$ $\{L_x$ = *trans*-$(CO)_2[P(OR)_3](dppm)$ (R = Et or Ph)} are best prepared, as purple and blue solids respectively, by adding $Ag[PF_6]$ to the mononuclear $Mn^{II}$ salts *trans*-$[Mn(CN)(CO)_2\{P(OR)_3\}(dppm)][PF_6]$ {preformed by $[N(C_6H_4Br\text{-}p)_3][PF_6]$ oxidation of the $Mn^{I}$ complex} in a 1:2 molar ratio in $CH_2Cl_2$. It seems likely, therefore, that the trications are formed from *cis*- or *trans*-$[Mn(CN)(CO)_2\{P(OR)_3\}(dppm)]$ in a stepwise reaction involving $Ag^+$ oxidation of the $Mn^{I}$ ligand to the $Mn^{II}$ cation which then co-ordinates to $Ag^+$. The alternative reaction sequence, in which $Ag^+$ co-ordination to $Mn^{I}$ is followed by $Ag^+$ oxidation of the trinuclear monocation to the trication, is less likely. While $[Ag\{(\mu\text{-NC})MnL_x\}_2]^+$ $\{L_x$ = *trans*-$(CO)_2[P(OPh)_3](dppm)\}$ is oxidised to the trication by $Ag[PF_6]$, the isomer $[Ag\{(\mu\text{-NC})MnL_x\}_2]^+$ $\{L_x$ = *cis*-$(CO)_2[P(OPh)_3](dppm)\}$, with a higher oxidation potential, is not (and note that all of the silver complexes are oxidised at higher potentials than are the mononuclear $Mn^{I}$ ligands).

Once formed from $Ag^+$ and $[Ag\{(\mu\text{-NC})MnL_x\}_2]^+$, $[Ag\{(\mu\text{-NC})MnL_x\}_2]^{3+}$ slowly decays to $[Ag\{(\mu\text{-NC})MnL_x\}_2]^+$ $\{L_x$ = *cis*-$(CO)_2[P(OPh)_3](dppm)\}$. Isomerisation is also observed when $[Ag\{(\mu\text{-NC})MnL_x\}_2]^{3+}$ and $[Ag\{(\mu\text{-NC})MnL_x\}_2]^+$ $\{L_x$ = *trans*-$(CO)_2[P(OPh)_3](dppm)\}$ are mixed in a 1:1 ratio (in an attempt to generate the mixed valence dication $[Ag\{(\mu\text{-NC})MnL_x\}_2]^{2+}$); the product mixture contains $[Ag\{(\mu\text{-NC})MnL_x\}_2]^{3+}$ and $[Ag\{(\mu\text{-NC})MnL_x\}_2]^+$ $\{L_x$ = *cis*-$(CO)_2[P(OPh)_3(dppm)\}$. Moreover, $[Ag\{(\mu\text{-NC})MnL_x\}_2]^+$ is isomerised to the *cis* form by catalytic amounts (10 mol %) of either $[Ag\{(\mu\text{-NC})MnL_x\}_2]^{3+}$ $\{L_x$ = *trans*-$(CO)_2[P(OPh)_3](dppm)\}$ or the free $Mn^{II}$ cation *trans*-$[Mn(CN)(CO)_2\{P(OPh)_3\}(dppm)]^+$ (a reaction better defined for the catalysed conversion of *trans*-$[Mn(CN)(CO)_2\{P(OPh)_3\}(dppm)]$ to its *cis* isomer [9]).

As described above, the voltammetry of the gold complexes $[Au\{(\mu\text{-NC})MnL_x\}_2]^+$ $\{L_x$ = *trans*-$(CO)_2[P(OR)_3](dppm)$ (R = Et or Ph)} is very different from that of the copper and silver analogues and suggests that one-electron oxidation should result in a Class II mixed-valence dication.[10] The IR spectrum of the dark yellow solution formed by electrolytic oxidation of $[Au\{(\mu\text{-NC})MnL_x\}_2]^+$ $\{L_x$ = *trans*-$(CO)_2[P(OEt)_3](dppm)\}$ in thf (see above) shows two carbonyl bands, at 2001 and 1931 $cm^{-1}$, and two cyanide bands, at 2165 and 2091 $cm^{-1}$. A very similar spectrum is observed (carbonyl bands at 2004 and 1928, cyanide bands at 2163 and 2096 $cm^{-1}$) when $[Au\{(\mu\text{-NC})MnL_x\}_2]^+$ $\{L_x$ = *trans*-$(CO)_2[P(OEt)_3](dppm)\}$ is treated with 1 equivalent of $[N(C_6H_4Br\text{-}p)_3][PF_6]$ or $[Fe(\eta\text{-}C_5H_4COMe)(cp)][PF_6]$ in $CH_2Cl_2$, suggesting the same species to be formed by chemical oxidation. Addition of the one-electron reductant $[Co(cp)_2]$ to the dark yellow solution regenerated the monocation $[Au\{(\mu\text{-NC})MnL_x\}_2]^+$ $\{L_x$ = *trans*-$(CO)_2[P(OEt)_3](dppm)\}$ quantitatively, providing additional evidence for the formation of the dication $[Au\{(\mu\text{-NC})MnL_x\}_2]^{2+}$ $\{L_x$ = *trans*-$(CO)_2[P(OEt)_3](dppm)\}$. Treatment of the solution of the dication with a second equivalent of $[N(C_6H_4Br\text{-}p)_3][PF_6]$ gave a red solution with a weak cyanide band at 2174 $cm^{-1}$ and one strong carbonyl band at 2006 $cm^{-1}$.

The changes in the IR spectrum on oxidation of $[Au\{(\mu\text{-NC})MnL_x\}_2]^+$ $\{L_x$ = *trans*-$(CO)_2[P(OEt)_3](dppm)\}$ suggest the formation of a dication in which the unpaired electron is localised on one manganese atom (Class I behaviour). Thus, the band at 2004 $cm^{-1}$ is typical of a *trans*-$Mn^{II}(CO)_2L(L–L)$ fragment and that at 1928 $cm^{-1}$ of *trans*-$Mn^{I}(CO)_2L(L–L)$. Though this would seem to contradict the voltammetric results, which suggest some interaction between the two redox-active sites, the time-scales of the two techniques (cyclic voltammetry and IR spectroscopy) are very different. Thus, the IR spectra

are not incompatible with Class II mixed-valence behaviour on the cyclic voltammetric time-scale.

The changes in ν(CN) when a terminal cyanide ligand acts as a bridge to a second metal site have been discussed recently, the energy of the vibration depending on kinematic effects [the constraint on motion resulting from N attachment of a second metal centre acts to increase ν(CN)] and the π-bonding abilities of the metal centres attached to the C and N termini of the cyanide bridge.[11,12] That one of the cyanide absorptions observed on oxidation (at 2096 $cm^{-1}$) is *ca.* 5 $cm^{-1}$ *lower* in energy than that of the monocation $[Au\{(\mu\text{-}NC)MnL_x\}_2]^+$ $\{L_x$ = *trans*-$(CO)_2[P(OEt)_3](dppm)\}$ is consistent with the formation of the $Mn^I$–NC–Au–NC–$Mn^{II}$ core; as found previously,[1b,13] oxidation at the M′ end of a complex containing a M(μ-CN)M′ skeleton leads to a decrease in energy of ν(CN). By contrast, oxidation at the $Mn^I$ terminus of a $Mn^I$(μ-CN)M′ unit leads to an increase in the energy of the CN stretching vibration. An increase of the order of 30–40 $cm^{-1}$,[1b,3] is found on oxidation of $[Ag\{(\mu\text{-}NC)MnL_x\}_2]^+$ $\{L_x$ = *trans*-$(CO)_2[P(OEt)_3](dppm)\}$ to $[Ag\{(\mu\text{-}NC)MnL_x\}_2]^{3+}$ $\{L_x$ = *trans*-$(CO)_2[P(OEt)_3](dppm)\}$ (Table 1). However, the shift of 60 $cm^{-1}$, to 2163 $cm^{-1}$, on one-electron oxidation of $[Au\{(\mu\text{-}NC)MnL_x\}_2]^+$ $\{L_x$ = *trans*-$(CO)_2[P(OEt)_3](dppm)\}$ is higher than observed for any other complex containing the $Mn^{II}$ ligands described herein. (Note that ν(CN) for the proposed trication $[Au\{(\mu\text{-}NC)MnL_x\}_2]^{3+}$ $\{L_x$ = *trans*-$(CO)_2[P(OEt)_3](dppm)\}$ is higher still, at 2174 $cm^{-1}$; *cf.* 2143 $cm^{-1}$ for $[Ag\{(\mu\text{-}NC)MnL_x\}_2]^{3+}$ $\{L_x$ = *trans*-$(CO)_2[P(OEt)_3](dppm)\}$.)

The shift in ν(CN) when $[Au\{(\mu\text{-}NC)MnL_x\}_2]^+$ $\{L_x$ = *trans*-$(CO)_2[P(OEt)_3](dppm)\}$ is oxidised to the dication seems unusually large. As noted above, although the IR carbonyl spectra are compatible with a trapped-valence dication, the electrochemical results suggest Class II character. Different spectroscopic behaviour related to the Mn–CN–M′–NC–Mn bridge may therefore be expected between the gold and silver analogues. A second possibility, involving isomerisation of one or both of the μ-CN bridges, *e.g.* of Mn–CN–Au–NC–Mn to Mn–NC–Au–NC–Mn, cannot be ruled out. Thermal isomerisation of $[(Ph_3P)Au(\mu\text{-}CN)RhCl_2(PMe_2Ph)_3][ClO_4]$ to $[(Ph_3P)Au(\mu\text{-}NC)RhCl_2(PMe_2Ph)_3][ClO_4]$ has, indeed, been observed.[14] However, we have not previously seen such behaviour in complexes derived from $Mn^I$ and $Mn^{II}$ cyanocarbonyl complex ligands, and others have also noted[15] that cyanide-bridged organometallics seem remarkably robust towards rearrangement of the M(μ-CN)M′ core.

## Conclusion

A wide range of linear trimetallic complexes $[M\{(\mu\text{-}NC)MnL_x\}_2]^+$ {M = Cu, Ag or Au; $L_x$ = *cis*- or *trans*-$(CO)_2[P(OR)_3](dppm)$ (R = Ph or Et), *cis*-$(CO)_2(PEt_3)(dppe)$ or $(CO)(dppm)_2$} has been synthesised. The marked differences in voltammetric behaviour between the gold complexes $[Au\{(\mu\text{-}NC)MnL_x\}_2]^+$ $\{L_x$ = *trans*-$(CO)_2[P(OR)_3](dppm)$ and $(CO)(dppm)_2\}$ lend further support to the suggestion that intramolecular electron transfer between the two redox-active centres depends on the arrangement of the ancillary ligand set at manganese. Furthermore, the *trans* disposition of the ligands at gold in $[Au\{(\mu\text{-}NC)MnL_x\}_2]^+$ $\{L_x$ = *trans*-$(CO)_2[P(OR)_3](dppm)\}$ facilitates intramolecular interaction when compared with $[Rh(CO)_2\{(\mu\text{-}NC)MnL_x\}_2][PF_6]$ $\{L_x$ = *trans*-$(CO)_2[P(OR)_3](dppm)$ (R = Et or Ph), *cis* geometry at square planar $Rh^I\}$. Surprisingly, the complexes $[M\{(\mu\text{-}NC)MnL_x\}_2]^+$ {M = Cu or Ag, $L_x$ = *trans*-$(CO)_2[P(OR)_3](dppm)\}$ show no evidence for interaction between the two manganese sites on oxidation. The extent to which intramolecular electron transfer depends on the bridging atom M will be further studied by means of MO calculations.

## Experimental

The preparation, purification and reactions of the complexes described were carried out under an atmosphere of dry nitrogen or argon using dried, distilled and deoxygenated solvents; reactions were monitored by IR spectroscopy where appropriate. Unless stated otherwise complexes were purified by dissolution in $CH_2Cl_2$ or thf, filtration of the solution through Celite, addition of *n*-hexane to the filtrate and reduction of the volume of the mixture *in vacuo* to induce precipitation. The compounds $[Cu(NCMe)_4][PF_6]$,[16] $[N(C_6H_4Br\text{-}p)_3][PF_6]$,[17] $[Fe(cp)_2][PF_6]$,[4b,18] $[Fe(\eta\text{-}C_5H_4COMe)(cp)][PF_6]$,[4b,19] [Au-Cl(tht)],[20] *cis*- and *trans*-$[Mn(CN)(CO)_2\{P(OR)_3\}(dppm)]$ (R = Et[1a] or Ph[21]), *cis*-$[Mn(CN)(CO)_2(PEt_3)(dppe)]$,[1a] and *trans*-$[Mn(CN)(CO)_2(PR_3)(L\text{–}L)][PF_6]$ (R = OEt or OPh, L–L = dppm; R = Et, L–L = dppe),[5] *trans*-$[Mn(CN)(CO)(dppm)_2]$ and *trans*-$[Mn(CN)(CO)(dppm)_2][PF_6]\cdot CH_2Cl_2$[1b] were prepared by published methods. Silver(I) salts were purchased from Aldrich. Infrared spectra were recorded on a Nicolet 5ZDX FT spectrometer. X-Band ESR spectra were recorded on a Bruker ESP-300E spectrometer equipped with a Bruker variable-temperature accessory and a Hewlett-Packard 5350B microwave frequency counter. The field calibration was checked by measuring the resonance of the diphenylpicrylhydrazyl (dpph) radical before each series of spectra. Fast atom bombardment (FAB) mass spectra were recorded on a Fisons Autospec instrument. Bulk magnetic susceptibility measurements were carried out at room temperature using a Sherwood Scientific magnetic susceptibility balance. Electrochemical studies were carried out using an EG&G model 273 potentiostat in conjunction with a three-electrode cell. For cyclic voltammetry the auxiliary electrode was a platinum wire and the working electrode a platinum disc. The reference was an aqueous saturated calomel electrode (SCE) separated from the test solution by a fine-porosity frit and an agar bridge saturated with KCl. Solutions were $0.1 \times 10^{-3}$ mol $dm^{-3}$ or $5 \times 10^{-4}$ mol $dm^{-3}$ in the test compound and 0.1 mol $dm^{-3}$ in $[NBu_4][PF_6]$ as the supporting electrolyte. Under these conditions, $E^{o\prime}$ for the one-electron oxidation of $[Fe(cp)_2]$ and $[Fe(\eta\text{-}C_5Me_5)_2]$, added to the test solutions as internal calibrants, are 0.47 and −0.09 V respectively in $CH_2Cl_2$. Microanalyses were carried out by the staff of the Microanalytical Service of the School of Chemistry, University of Bristol.

### Syntheses

**$[Cu\{(\mu\text{-}NC)MnL_x\}_2][PF_6]$ $\{L_x$ = *trans*-$(CO)_2[P(OEt)_3](dppm)\}$.** To a stirred solution of *trans*-$[Mn(CN)(CO)_2\{P(OEt)_3\}(dppm)]$ (100 mg, 0.145 mmol) in $CH_2Cl_2$ (20 $cm^3$) was added $[Cu(NCMe)_4][PF_6]$ (27 mg, 0.073 mmol). After 5 min the yellow solution was filtered and *n*-hexane added. Partial removal of the solvent *in vacuo* gave an oily yellow solid which was triturated with diethyl ether and then purified from $CH_2Cl_2$–diethyl ether to give the product as a yellow solid, yield 90 mg (78%).

The complexes $[Cu\{(\mu\text{-}NC)MnL_x\}_2][PF_6]$ $\{L_x$ = *cis*-$(CO)_2[P(OR)_3](dppm)$ (R = Et or Ph), *trans*-$(CO)_2[P(OPh)_3](dppm)$ and $(CO)(dppm)_2\}$ were prepared similarly.

**$[Ag\{(\mu\text{-}NC)MnL_x\}_2][PF_6]$ $\{L_x$ = *trans*-$(CO)_2[P(OEt)_3](dppm)\}$.** To a stirred solution of *trans*-$[Mn(CN)(CO)_2\{P(OEt)_3\}(dppm)]$ (100 mg, 0.145 mmol) in toluene (10 $cm^3$) was added dropwise a solution of $Ag[PF_6]$ (180 mg, 0.073 mmol) in toluene (10 $cm^3$). After 15 min the yellow solution was reduced in volume to *ca.* 5 $cm^3$ and then *n*-hexane was added to precipitate a pale yellow solid. The solid was washed with toluene and then *n*-hexane and purified from $CH_2Cl_2$–diethyl ether to give the yellow product, yield 80 mg (67%).

The complexes $[Ag\{(\mu\text{-}NC)MnL_x\}_2][PF_6]$ $\{L_x$ = *cis*- or *trans*-$(CO)_2[P(OPh)_3](dppm)\}$ were prepared similarly.

**Table 5** Details of the crystal-structure determinations

| | $[Ag\{(\mu\text{-}NC)MnL_x\}_2][PF_6]\cdot 2OEt_2$ $\{L_x = trans\text{-}(CO)_2[P(OPh)_3](dppm)\}$ | $[Au\{(\mu\text{-}NC)MnL_x\}_2][PF_6]\cdot 1.25CH_2Cl_2$ $\{L_x = trans\text{-}(CO)_2[P(OEt)_3](dppm)\}$ | $[Ag\{(\mu\text{-}NC)Mn(CO)(dppm)_2\}_2][PF_6]_3\cdot 4CH_2Cl_2$ |
|---|---|---|---|
| Crystal data | | | |
| Empirical formula | $C_{100}H_{94}AgF_6Mn_2N_2O_{12}P_7$ | $C_{69.25}H_{76.5}AuCl_{2.5}F_6Mn_2N_2O_{10}P_7$ | $C_{108}H_{96}AgCl_8F_{18}Mn_2N_2O_2P_{11}$ |
| $M$ | 2064.31 | 1823.09 | 2637.88 |
| Crystallisation solvent ($T$/°C) | $CH_2Cl_2$–$OEt_2$ (−10) | $CH_2Cl_2$–*n*-hexane (−10) | $CH_2Cl_2$–cyclohexane (−10) |
| Crystal size/mm | 0.70 × 0.30 × 0.30 | 0.50 × 0.30 × 0.25 | 0.40 × 0.30 × 0.20 |
| Crystal system | Triclinic | Monoclinic | Monoclinic |
| Space group | $P\bar{1}$ (no. 2) | $P2_1/c$ (no. 14) | $P2_1/c$ (no. 14) |
| $a$/Å | 10.023(2) | 19.046(13) | 19.293(4) |
| $b$/Å | 13.003(3) | 21.993(9) | 15.096(4) |
| $c$/Å | 20.135(4) | 21.641(10) | 20.752(4) |
| α/° | 83.20(3) | | |
| β/° | 82.83(3) | 105.36(5) | 96.359(12) |
| γ/° | 76.58(3) | | |
| $U$/Å$^3$ | 2521.7(9) | 8741(8) | 6007(2) |
| $Z$ | 1 | 4 | 2 |
| $D_c$/Mg m$^{-3}$ | 1.359 | 1.385 | 1.458 |
| μ/mm$^{-1}$ | 0.619 | 2.225 | 0.768 |
| $F$(000) | 1060 | 3666 | 2668 |
| Data collection and reduction | | | |
| $T$/K | 293(2) | 293(2) | 298(2) |
| Scan type | Wyckoff, ω | Wyckoff, ω | ω |
| Index ranges | $0 \leqslant h \leqslant 11, -15 \leqslant k \leqslant 15, -23 \leqslant l \leqslant 23$ | $0 \leqslant h \leqslant 22, 0 \leqslant k \leqslant 26, -25 \leqslant l \leqslant 24$ | $0 \leqslant h \leqslant 9, 0 \leqslant k \leqslant 17, -24 \leqslant l \leqslant 24$ |
| Reflections collected | 9273 | 8467 | 6098 |
| Unique reflections with $I > -3\sigma(I)$ ($n_o$) | 8707 | 8018 | 5759 |
| $R_{int}$ | 0.0223 | 0.0520 | 0.0876 |
| Reflections with $I > 2\sigma(I)$ | 5471 | 3685 | 1525 |
| No. azimuthal scan data | 259 | 878 | *a* |
| Min., max. transmission coefficients | 0.278, 0.343 | 0.691, 1.00 | *a* |
| Solution and refinement | | | |
| Least-squares variables | 627 | 580 | 304 |
| Least-squares restraints | 41 | 123 | 50 |
| $g$,$h$ | 0.10, 10 | 0.10, 0.0 | 0.15, 0.0 |
| Non-H atoms: | | | |
| thermal params. aniso. | All | All but carbons | Ag, Mn, P, F, solvent |
| thermal params. iso. | None | Carbons | All others |
| Disorder | Solvent atoms, O(4), O(6) | Solvent atoms | Solvent, anions |
| Final $R$ indices[b] | $R1$ 0.0780, $wR2$ 0.188 | $R1$ 0.0950, $wR2$ 0.2053 | $R1$ 0.0981, $wR2$ 0.2422 |
| Goodness-of-fit, $S$[b] | 1.041 | 1.148 | 0.811 |
| $E_{max}$, $E_{min}$/e Å$^{-3}$ | 0.72, −0.80 | 0.84, −0.70 | 0.859, −0.496 |

[a] Undefined, crystal decomposed. [b] Residuals calculated for reflections with $I > 2\sigma(I)$; $wR2 = [\Sigma w\Delta^2/\Sigma wF_o^4]^{\frac{1}{2}}$; $S = [\Sigma w\Delta^2/(n - n_v)]^{\frac{1}{2}}$; $R1 = \Sigma||F_o| - |F_c||/\Sigma|F_o|$; $\Delta = F_o^2 - F_c^2$; $n = n_o$ + restraints; $w = [\sigma_c^2(F_o^2) + (gP)^2 + hP]^{-1}$, $\sigma_c^2(F_o^2)$ = variance in $F_o^2$ due to counting statistics, $P = [\max(F_o^2,0) + 2F_c^2]/3$.

**$[Ag\{(\mu\text{-}NC)MnL_x\}_2][PF_6]_3$ $\{L_x$ = *trans*-$(CO)_2[P(OEt)_3]$-(dppm)}.** To a stirred solution of *cis*-$[Mn(CN)(CO)_2\{P(OEt)_3\}$-(dppm)] (125 mg, 0.182 mmol) in $CH_2Cl_2$ (20 cm$^3$) was added $[N(C_6H_4Br\text{-}p)_3][PF_6]$ (114 mg, 0.182 mmol). The resulting red solution was filtered and then solid $Ag[PF_6]$ (23 mg, 0.091 mmol) was added. After stirring the mixture for 5 min the purple solution was filtered, *n*-hexane (25 cm$^3$) was added, and the volume of the solution was reduced *in vacuo* to give an oily precipitate. Purification from $CH_2Cl_2$–diethyl ether gave the product as a purple solid, yield 90 mg (51%).

The complex $[Ag\{(\mu\text{-}NC)MnL_x\}_2][PF_6]_3$ $\{L_x$ = *trans*-$(CO)_2[P(OPh)_3](dppm)\}$ was prepared similarly.

**$[Ag\{(\mu\text{-}NC)MnL_x\}_2][PF_6]_3$ $[L_x$ = *trans*-$(CO)(dppm)_2]$.** To a stirred solution of *trans*-$[Mn(CN)(CO)(dppm)_2]$ (234 mg, 0.27 mmol) in $CH_2Cl_2$ (25 cm$^3$) was added $Ag[PF_6]$ (167 mg, 0.66 mmol). After 5 min the deep red solution was filtered, *n*-hexane was added, and the volume of the solvent was reduced *in vacuo* to give a deep red solid which was purified from $CH_2Cl_2$–*n*-hexane, yield 126 mg (41%).

The complex $[Ag\{(\mu\text{-}NC)MnL_x\}_2][PF_6]_3$ $[L_x$ = *trans*-$(CO)_2(PEt_3)(dppe)]$ was prepared similarly from *cis*-$[Mn(CN)(CO)_2(PEt_3)(dppe)]$ and $Ag[PF_6]$.

**$[Au\{(\mu\text{-}NC)MnL_x\}_2][PF_6]$ $\{L_x$ = *trans*-$(CO)_2[P(OEt)_3]$-(dppm)}.** To a stirred solution of *trans*-$[Mn(CN)(CO)_2$-$\{P(OEt)_3\}(dppm)]$ (75 mg, 0.109 mmol) in $CH_2Cl_2$ (30 cm$^3$) was added [AuCl(tht)] (17 mg, 0.051 mmol). After stirring the mixture for 5 min $Tl[PF_6]$ (19 mg, 0.051 mmol) was added and stirring was continued for 3 h. After filtration the reaction mixture was reduced in volume *in vacuo*, layered with *n*-hexane and allowed to crystallise at −10 °C. Purification by the same method gave the product as yellow crystals, yield 52 mg (56%).

The complexes $[Au\{(\mu\text{-}NC)MnL_x\}_2][PF_6]$ $\{L_x$ = *cis*-$(CO)_2[P(OR)_3](dppm)$ (R = Et or Ph), *trans*-$(CO)_2$-$[P(OPh)_3](dppm)$ or $(CO)(dppm)_2\}$ were prepared similarly.

**$[Au\{(\mu\text{-}NC)MnL_x\}_2][PF_6]_3$ $[L_x$ = *trans*-$(CO)(dppm)_2]$.** To a stirred solution of $[Au\{(\mu\text{-}NC)MnL_x\}_2][PF_6]$ $[L_x$ =

$(CO)(dppm)_2$] (37 mg, 0.018 mmol) in $CH_2Cl_2$ (20 $cm^3$) was added $[Fe(cp)_2][PF_6]$ (12 mg, 0.035 mmol). After 2 h the red solution was filtered through Celite and *n*-hexane was added to precipitate a red solid. Purification from $CH_2Cl_2$–*n*-hexane gave the product, yield 30 mg (73%).

### Structure determinations of $[Ag\{(\mu\text{-NC})MnL_x\}_2][PF_6]\cdot 2OEt_2$ {$L_x$ = *trans*-$(CO)_2[P(OPh)_3](dppm)$}, $[Au\{(\mu\text{-NC})MnL_x\}_2][PF_6]\cdot 1.25CH_2Cl_2$ {$L_x$ = *trans*-$(CO)_2[P(OEt)_3](dppm)$} and $[Ag\{(\mu\text{-NC})Mn(CO)(dppm)_2\}_2][PF_6]_3\cdot 4CH_2Cl_2$

Many of the details of the structure analyses are listed in Table 5. X-Ray diffraction measurements on single crystals mounted in thin-walled glass capillaries were made with graphite-monochromated Mo-K$\alpha$ X-radiation ($\bar{\lambda}$ = 0.710 73 Å) using Siemens four-circle R3m or P4 diffractometers. In all three cases crystal quality was less than optimum with weak diffraction and poor crystallinity generally observed. Samples chosen for study were the best of many assessed.

Intensity data were collected for unique portions of reciprocal space and corrected for Lorentz and polarisation effects, long-term intensity fluctuations, and for absorption effects (on the basis of azimuthal scan data). The structures were solved by direct methods, and refined by full-matrix least squares against $F^2$ for all data with $I > -3\sigma(I)$ with weights, $w$, set equal to $[\sigma_c^2(F_o^2) + (gP)^2 + hP]^{-1}$, where $P = [\max(F_o^2, 0) + 2F_c^2]/3$ and $g$ and $h$ were assigned values given in Table 5. All non-hydrogen atoms were refined without positional constraints except as follows: in $[Ag\{(\mu\text{-NC})MnL_x\}_2][PF_6]\cdot 2OEt_2$, phenyl rings were restrained to be close to planar and the silver atom of the cation lies at an inversion centre; in $[Ag\{(\mu\text{-NC})Mn(CO)(dppm)_2\}_2][PF_6]_3\cdot 4CH_2Cl_2$ phenyl rings were constrained to local $D_{6h}$ symmetry (C–C 1.395 Å), the anions were constrained to octahedral symmetry with P–F 1.51 Å and the silver atom of the cation lies at an inversion centre. The structures are highly disordered. In $[Ag\{(\mu\text{-NC})Mn(CO)(dppm)_2\}_2][PF_6]_3\cdot 4CH_2Cl_2$ the anions occupy two crystallographically distinct sites of occupancy 85.2 and 64.8% (summing to 150% to balance the charge of the 50% of the cation that is crystallographically unique). In $[Ag\{(\mu\text{-NC})MnL_x\}_2][PF_6]\cdot 2OEt_2$ the diethyl ether molecules are disordered about inversion centres and one OPh group shows two sites for oxygen [O(4) 83 and O(6) 17%]; in $[Au\{(\mu\text{-NC})MnL_x\}_2][PF_6]\cdot 1.25CH_2Cl_2$ there are three distinct solvent sites each of 50% occupancy, one disordered about an inversion centre. All hydrogen atoms were assigned isotropic displacement parameters and were constrained to ideal geometries. Final difference syntheses showed no chemically significant features; the largest remaining features are close to the anion or solvent atoms. Refinements converged to residuals given in Table 5. All calculations were made with programs of the SHELXTL-PLUS system.[22] Complex neutral-atom scattering factors were taken from ref. 23.

Atomic coordinates, thermal parameters, and bond lengths and angles have been deposited at the Cambridge Crystallographic Data Centre (CCDC). See Instructions for Authors, *J. Chem. Soc., Dalton Trans.*, 1996, Issue 1. Any request to the CCDC for this material should quote the full literature citation and the reference number 186/185.


## Acknowledgements

We thank the EPSRC for a Research Studentship (to N. C. B.), a Research Assistantship (to G. H. W) and funds to purchase an ESR spectrometer. One of us (A. M.) thanks the Spanish Ministerio de Educacion y Ciencia for a F.P.U. (Becas en el extranjero) grant.


## References


1 (*a*) G. A. Carriedo, N. G. Connelly, M. C. Crespo, I. C. Quarmby, V. Riera and G. H. Worth, *J. Chem. Soc., Dalton Trans.*, 1991, 315; (*b*) A. Christofides, N. G. Connelly, H. J. Lawson, A. C. Loyns, A. G. Orpen, M. O. Simmonds and G. H. Worth, *J. Chem. Soc., Dalton Trans.*, 1991, 1595; (*c*) G. A. Carriedo, N. G. Connelly, S. Alvarez, E. Perez-Carreno and S. Garcia-Granda, *Inorg. Chem.*, 1993, **32**, 272; (*d*) M. Bardaji, N. C. Brown, A. Christofides and N. G. Connelly, *J. Organomet. Chem.*, 1994, **474**, C24.

2 G. A. Carriedo, N. G. Connelly, E. Perez-Carreno, A. G. Orpen, A. L. Rieger, P. H. Rieger, V. Riera and G. M. Rosair, *J. Chem. Soc., Dalton Trans.*, 1993, 3103.

3 F. L. Atkinson, A. Christofides, N. G. Connelly, H. J. Lawson, A. C. Loyns, A. G. Orpen, G. M. Rosair and G. H. Worth, *J. Chem. Soc., Dalton Trans.*, 1993, 1441.

4 (*a*) P. K. Baker, K. Broadley, N. G. Connelly, B. A. Kelly, M. D. Kitchen and P. Woodward, *J. Chem. Soc., Dalton Trans.*, 1980, 1710; (*b*) N. G. Connelly and W. E. Geiger, *Chem. Rev.*, 1996, **96**, 877.

5 N. G. Connelly, K. A. Hassard, B. J. Dunne, A. G. Orpen, S. J. Raven, G. A. Carriedo and V. Riera, *J. Chem. Soc., Dalton Trans.*, 1988, 1623.

6 P. G. Jones, H. W. Roesky and J. Schimkowiak, *J. Chem. Soc., Chem. Commun.*, 1988, 730.

7 H. W. Roesky, J. Schimkowiak, K. Meyer-Base and P. G. Jones, *Angew. Chem., Int. Ed. Engl.*, 1986, **25**, 1006.

8 H. W. Roesky, J. Schimkowiak, P. G. Jones, M. Noltemeyer and G. M. Sheldrick, *J. Chem. Soc., Dalton Trans.*, 1988, 2507.

9 N. G. Connelly, S. J. Raven, G. A. Carriedo and V. Riera, *J. Chem. Soc., Chem. Commun.*, 1986, 992.

10 M. B. Robin and P. Day, *Adv. Inorg. Chem. Radiochem.*, 1967, **10**, 247.

11 C. A. Bignozzi, R. Argazzi, J. R. Schoonover, K. C. Gordon, R. B. Dyer and F. Scandola, *Inorg. Chem.*, 1992, **31**, 5260.

12 D. H. Johnston, C. L. Stern and D. F. Shriver, *Inorg. Chem.*, 1993, **32**, 5170.

13 N. Zhu and H. Vahrenkamp, *J. Organomet. Chem.* 1994, **472**, C5.

14 A. J. Deeming, G. P. Proud, H. M. Dawes and M. B. Hursthouse, *Polyhedron*, 1988, **7**, 651.

15 N. Zhu and H. Vahrenkamp, *Angew. Chem., Int. Ed. Engl.*, 1994, **33**, 2090.

16 G. J. Kubas, *Inorg. Synth.*, 1990, **28**, 68.

17 F. A. Bell, A. Ledwith and D. C. Sherrington, *J. Chem. Soc. C.*, 1969, 2719.

18 J. C. Smart and B. L. Pinsky, *J. Am. Chem. Soc.*, 1980, **102**, 1009.

19 C. Guillon and P. Vierling, *J. Organomet. Chem.*, 1994, **464**, C42.

20 R. Uson, A. Laguna and M. Laguna, *Inorg. Synth.*, 1989, **26**, 86.

21 G. A. Carriedo, M. C. Crespo, V. Riera, M. G. Sanchez, M. L. Valin, D. Moreiras and X. Solans, *J. Organomet. Chem.*, 1986, **302**, 47.

22 G. M. Sheldrick, SHELXTL PLUS, Revision 5, University of Göttingen, 1995.

23 *International Tables for Crystallography*, Kluwer, Dordrecht, 1992, vol. C.



*Received* 10*th May* 1996; *Paper* 6/03273G